Revista Mexicana de Ingeniería Química

Effect of spray-drying conditions on moisture content and particle size of coffee extract in a prototype dryer

Efecto de las condiciones del secado por aspersión sobre el contenido de humedad y tamaño de partícula de extracto de café en un secador prototipo

J. Villegas-Santiago[1], F. Gómez-Navarro[1], A. Domínguez-Niño[1], M.A. García-Alvarado[2], M.A. Salgado-Cervantes[2] and G. Luna-Solano[1]*

[1]*Instituto Tecnológico de Orizaba. Av. Oriente 9 Núm. 852 Col. Emiliano Zapata, C.P. 94320, Orizaba, Veracruz, México.*
[2]*Instituto Tecnológico de Veracruz, Departamento de Ingeniería Química y Bioquímica. Av. Miguel Ángel de Quevedo No. 2779,91897, Veracruz, Veracruz, México.*

Abstract

In this work, the effect of spray drying conditions on the moisture content and particle size of coffee extract was studied. The factors investigated were the inlet temperature (150 to 220 °C), air flow (537 to 691 kg·h^{-1}), and frequency of the rotary atomizer (60 to 90 Hz). An analysis of variance revealed that the independent variables had significant effects ($p < 0.10$) on the response variables. An increase in the frequency of the rotary atomizer from 60 to 90 Hz produced an increase in the outlet temperature and, therefore, a decrease in the product moisture content. The luminosity of the powders increased as the inlet temperature and air flow increased from 150 to 220 °C and from 537 to 691 kg·h^{-1}, respectively; therefore, the coffee powder turned brighter. A decrease in hysteresis was observed as the air flow rate increased from 537 to 691 kg·h^{-1}.

Keywords: Spray drying, coffee, particle size, sorption isotherms, GAB and BET model.

Resumen

En este trabajo se investigó el efecto de las condiciones del secado por aspersión sobre el contenido de humedad y tamaño de partícula de extracto de café. Los factores investigados fueron la temperatura de entrada (150 a 220 °C), flujo de aire (537 a 691 kg·h^{-1}) y la frecuencia del atomizador rotatorio (60 a 90 Hz). El análisis de varianza reveló que las variables independientes tuvieron efecto significativo ($p < 0.10$) sobre las variables de respuesta. Un incremento en la frecuencia del atomizador rotatorio de 60 Hz a 90 Hz produjo un aumento en la temperatura de salida y, por lo tanto, una disminución en el contenido de humedad del producto. La luminosidad del café en polvo incrementó a medida que la temperatura de entrada y el flujo de aire aumentaron de 150 °C a 220 °C y de 537 kg·h^{-1} a 691 kg·h^{-1}, respectivamente; por lo tanto, el café en polvo se tornó más luminoso. Una disminución en la histéresis fue observada con un incremento en la velocidad de flujo de aire de 537 a 691 kg·h^{-1}.

Palabras clave: Secado por aspersión, café, tamaño de partícula, isotermas de sorción, modelo de GAB y modelo de BET.

1 Introduction

Coffee is the second-most important commodity internationally, with a worldwide production of approximately 8.2 million tons per year (Burmester *et al*., 2011). The countries with the highest coffee production in 2013 were Brazil, Vietnam, and Indonesia with 3,000, 1,500, and 8,000 million tons, respectively. Currently, Mexico is among the top ten producers worldwide, with a production of approximately 200 million kilograms per year (Hernández *et al*., 2019). Coffee is not only traded in large quantities, but also comes in a multitude of different qualities, varieties, and forms. These include Arabica and Robusta, roasted or green, as well as instant and soluble (FAO, 2015). The spray drying process transforms a pumpable fluid feed into a dried product in a single operation. The fluid is atomized using a rotating wheel or a nozzle, and the spray of droplets is immediately exposed to a flow of a hot drying medium, usually air. The resulting rapid evaporation maintains a low droplet temperature, such that high drying air temperatures can be applied without affecting the product (Filková *et al*., 2014).

Spray drying is not only advantageous in terms of cost, but is also an attractive method for extending the shelf life of foods and allows the continuous mass production of dried products in short periods of time (Domínguez *et al*., 2018). Water sorption isotherms are curves describing the relation between the food water activity and its corresponding equilibrium moisture content at a given temperature (Faria *et al*., 2016). The Brunauer-Emmet-Teller (BET) isotherm is one of the most successful models to determine the monolayer moisture content for foods. The two constants obtained from the BET model are the monolayer moisture content, m_0, and the energy constant, C_s. The model generally holds only for a limited range of a_w; however, the BET monolayer concept as a point for the moisture stability of dry foods was found to be a reasonable guide to stability with respect to moisture content. It should be noted that this a_w range of applicability is between 0 and 0.55; above the upper limit, the results deviate from the straight line when plotted as a linear equation. The Guggenheim-Anderson-de Boer (GAB) isotherm in an improved version of the BET model for multilayer adsorption, which has been found to adequately represent experimental data in the a_w range of 0 to 0.95 for most foods of practical interest. The GAB and BET models are based on the same principles of monolayer coverage; however, the GAB model introduced an additional degree of freedom (an additional constant k), with which the model has greater versatility (Labuza and Altunakar, 2007). Although many studies have been conducted on the effects of the operating conditions of spray-dried foods (Roustapour *et al*., 2006; Huang and Mujumdar, 2008; Lantigua *et al*., 2011; Solval *et al*., 2012), and to predict the moisture sorption behavior in some foods such as banana (Yang

et al., 2008), green tea powder and green tea granules (Sinija and Mishra, 2008), pinhão (Thys *et al*. 2010), apricot (Djendoubi *et al*., 2012), nixtamalized maize flour (Ramírez *et al*., 2014), cheddar cheese (Khetra, *et al*., 2017), sucrose-calcium, (Pascual *et al*., 2017), information about the effects of drying conditions on the particle size and sorption isotherms of coffee extract has been largely overlooked. In this context, the aim of this work was to evaluate the effects of the temperature, air flow rate, and frequency of the rotary atomizer on the particle size and sorption isotherms of diluted extract of coffee Arabica.

2 Materials and methods

2.1 Raw material

Concentrated coffee extract was obtained from a coffee producer; the extract came from the leaching of roasted coffee. Diluted coffee extract obtained from the concentrated extract was used as raw material in this work. Table 1 shows the properties of the coffee extract used for the experimental tests.

2.2 Drying process

A prototype spray dryer (Model PSA5, VIBRASEC S.A.S., Colombia) was employed for the spray drying process. A schematic diagram of the spray dryer is shown in Fig. 1. A diaphragm pump was used to pump the coffee extract to a rotary atomizer with a maximum feed rate of 420 mL/min, and atomization was performed using the rotary atomizer with a maximum frequency of 107 Hz.

Table 1. Characterization of the coffee extract.

Analysis	Mean values ±standard deviation	
	Diluted extract	Concentrated extract
Moisture content (%)	$92.96^{0.02}$	$39.86^{0.04}$
Total solids (%)	$7.04^{0.02}$	$60.14^{0.04}$
Caffeine ($g \cdot l^{-1}$)	$2.75^{0.16}$	$24.38^{0.02}$
Viscosity (Pa·s)	$110^{2.82}$	$135^{1.41}$
Surface tension ($Dn \cdot cm^{-1}$)	$43.6^{0.67}$	$51^{0.91}$
L	$0.59^{0.04}$	$0.54^{0.02}$
a	$0.18^{0.01}$	$0.17^{0.01}$
b	$-0.69^{0.04}$	$-0.28^{0.05}$

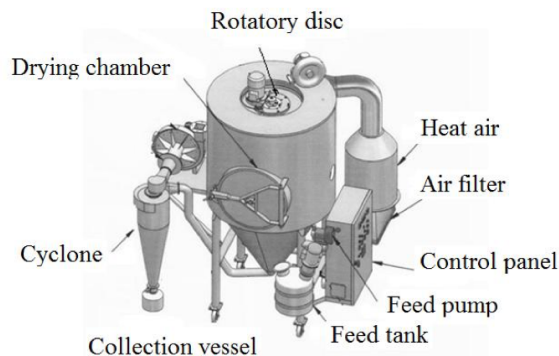*L* (Whiteness-Darkness), *a* (Greenness-Redness)
b (Yellowness-Blueness)

Fig. 1. Schematic illustration of pilot scale spray dryer.

2.3 Analytical methods

The product moisture content was measured with an infrared moisture balance (MB35, HALOGEN, OHAUS) at 105 °C, which contained a coffee extract sample of approximately 1 g. The results are expressed in terms of the dry basis (d.b). The water activity (a_w) of the coffee powder obtained during the drying process was determined at 25 °C using an Aqualab water activity meter (series 3 TE, DECAGON, Washington). The equipment was verified using verification standards of LiCl, NaCl, and KCl (salt solutions with a specific molality and water activity). The color of the samples was measured by a HunterLab (model MiniScan XE plus; Hunter Associates Laboratory, Retson, VA, USA) colorimeter. The equipment was calibrated with white and black standard tiles. The experimental color was determined by the reflectance mode and expressed in terms of the parameters L (whiteness-darkness), a (redness-greenness), and b (yellowness-blueness). The hue (H) and chroma (C) parameters were calculated using eqs. (1)-(2):

$$H = \tan^{-1}(b/a) \qquad (1)$$

$$C = (a^2 + b^2)^{1/2} \qquad (2)$$

The spray drying yield was calculated by determining the product recovery given by the percentage ratio of the total product mass recovered to the mass of extract fed to the system (Jiménez *et al.*, 2017).

In addition, the sorption isotherms were determined at 25 °C using an Aqualab automatic vapor sorption analyzer (VSA1033, DECAGON, USA). This method has been reported and used recently (Hernández *et al.*, 2019; Schmidt and Lee, 2012; Zhang *et al.*, 2017). The results were adjusted with BET and GAB models, as shown in eqs. (3)-(4), respectively.

$$M = \frac{m_0 \cdot C_s \cdot a_w}{(1 - a_w) \cdot (1 + (C_s - 1) \cdot a_w)} \qquad (3)$$

where M is the moisture content, kg water/kg dry mass; m_0 is the monolayer moisture content; C_s is a material constant related to heat sorption; and a_w is the water activity.

$$M = \frac{m_0 \cdot C_s \cdot k \cdot a_w}{(1 - k \cdot a_w) \cdot (1 + (C_s - 1) \cdot k \cdot a_w)} \qquad (4)$$

where M is the moisture content, kg water/kg dry mass; m_0 is the monolayer moisture content; C_s is the Guggenheim constant; k is a correction factor related to multilayer heat sorption; and a_w is the water activity.

2.4 Experimental design

A Box-Behnken design was adopted. In this design, three levels were required for each factor, with one central point, thus making the total number of experiments equal to 15 rather than 27 as with a full factorial design. The experiments were randomized to minimize the effects of unexplained variability in the observed responses as a result of external factors. Table 2 shows the independent variables used to determine the spray drying effects for coffee extract, including the coding symbols and codes. The experiments were conducted in duplicate, and the mean values are reported.

Table 2. Independent variables used in the coffee drying study.

Independent Variables	Symbol code	Coded variables		
		-1	0	+1
Inlet air temperature (°C)	X_1	150	185	220
Air flow (kg·h^{-1})	X_2	537	619	691
Frequency of the atomizer (Hz)	X_3	60	75	90

Table 3. Experimental data of coffee powder by spray drying.

	X_1	X_2	X_3	Outlet temperature (Y_1) °C	Moisture content (Y_2)%	Water activity (Y_3)	Color parameters			Yield Y_7(%)	Particle size $(Y_8)\mu$m
							Luminosity (Y_4)	Hue (Y_5)	Chroma (Y_6)		
1	-1	-1	-1	87	1.09	0.62	21.69	2.33	8.22	60	60
2	-1	1	-1	89	0.95	0.62	22.39	2.48	8.3	67	40
3	1	-1	-1	122	0.37	0.62	21.83	1.62	6.37	61	42.5
4	1	1	-1	124	0.39	0.62	21.86	2.21	7.4	87	60
5	-1	-1	1	95	0.9	0.62	25.53	3.96	11.22	93	50
6	-1	1	1	89	0.97	0.62	24.38	3.58	9.64	95	60
7	1	-1	1	140	1.85	0.62	24.84	3.11	9.44	85	95
8	1	1	1	132	0.91	0.62	28.08	3.91	10.03	82	40
9	0	0	0	103	2.5	0.176	23.41	1.2	5.25	80	55
10	0	1	0	119	2.06	0.062	21.89	1.12	5.65	82	45
11	0	-1	0	110	2.78	0.09	22.52	1.5	7.37	82	70
12	1	0	0	109	1.77	0.147	23.95	1.3	6.05	81	60
13	-1	0	0	101	2.61	0.263	23.85	1.03	6.29	80	50
14	0	0	1	103	2.19	0.221	23.55	0.61	5.34	86	50
15	0	0	-1	100	1.5	0.08	21.74	1.36	5.88	87	40

X_1= Inlet air temperature (°C); X_2= Air flow (kg·h^{-1}); X_3 Frequency of the atomizer (Hz).

The responses were the outlet air temperature (Y_1), final moisture content (Y_2), water activity (Y_3), luminosity (Y_4), hue (Y_5), chroma (Y_6), yield (Y_7), as well as particle size (Y_8) of the dried product (Table 3). Eight mathematical functions, $f(1,2,3,4,5,6,7,8)$, were assumed to exist for Y_k, as shown in Eq. (5):

$$Y_k = f_k(X_1, X_2, X_3) \qquad (5)$$

where X_1 is the inlet air temperature (°C), X_2 is the air flow (kg·h^{-1}), and X_3 is the frequency of the rotary atomizer (Hz). A second-degree polynomial equation of the form of Eq. (6) was used to approximate the function using the response surface methodology (RSM) of Minitab Release 16.

$$Y_k = b_{k0} + \sum_{i=1}^{3} b_{ki}X_i + \sum_{i=1}^{3} b_{kii}X_i^2 + \sum_{i \neq j=1}^{3} b_{kij}X_iX_j \quad (6)$$

where b_{k0}, b_{ki}, b_{kii}, and b_{kij} are the regression coefficients of the intercept, linear, quadratic, and interaction coefficients, respectively; the X_i s are the coded independent variables, which are linearly related to X_1, X_2, and X_3.

3 Results and discussion

The model coefficients obtained by regression for the second-order polynomials of the response surface of Y_1, Y_2, Y_3, Y_4, Y_5, Y_6, Y_7 and Y_8 are shown in Table 4. The results are represented with response surface models. The response surface plots for the dependent variables are shown in Fig. 2.

3.1 Outlet air temperature and moisture content

Fig. 2a shows the effects of the inlet air temperature, air flow, and frequency of the rotary atomizer on the outlet air temperature of the drying process. An analysis of variance (ANOVA) indicated that the inlet air temperature affected ($p \leq 0.10$) the outlet air temperature significantly. As seen from Fig. 2a, the highest outlet temperature occurred when the inlet air temperature increased from 150 to 220 °C. Likewise, the air flow increment had a direct impact on outlet temperature owing to the increase in the drying air flow rate, which decreased the residence time of the product in the drying chamber; as a result, an increment in the outlet temperature was observed.

Table 4. Regression coefficients of the polynomial equations representing the relationship of the response and the independent variables.

Coefficient	$K = 1$							
	Outlet temperature (Y_1) °C	Moisture content (Y_2) %	Water activity (Y_3)	Luminosity (Y_4)	Hue (Y_5)	Chroma (Y_6)	Yield (Y_7)	Particle size (Y_8) μm
b_{k0}	105	2.71	0.128	22.7	0.546	4.88	82.6	52
b_{k1}	9.29*	-0.432	-0.0357	0.272	-0.123	-0.438*	1.41	-5.11
b_{k2}	3.07	-0.047	0.0062*	0.219	0.078	-0.160*	3.67	-2.87
b_{k3}	4.67	0.314*	0.027	1.69*	0.517*	0.950*	5.65*	5.36
b_{k12}	-4.21	-0.261	-0.0111	0.465	0.202	0.39	1.17	-8.91
b_{k13}	10.4	0.463	0.0381	0.425	0.057	0.17	-4.45	11.2
b_{k23}	-5.5	-0.156	-0.0062	0.17	-0.04	-0.263	-6.79	-70.7
b_{k11}	-0.87	-0.578	0.0499	1.33	0.783	1.38	-2.81	3.69
b_{k22}	8.63	-0.348	-0.0786	-0.363	0.928	1.72	-1.31	6.19
b_{k33}	-4.37	-0.923	-0.0371	0.077	0.603	0.821	3.19	-6.31
R^2	0.87	0.93	0.78	0.67	0.82	0.88	0.8	0.52

* Significant at $p \leq 0.10$

b_{k0}, b_{ki}, b_{kii}, b_{kij} are regression coefficients for intercept, linear, quadratic and interaction coefficients respectively.

According to Goula and Adamopoulos, (2004), the movement of air predetermines the rate and degree of droplet evaporation by influencing the passage of the spray through the drying zone, the concentration of the product in the region of the dryer walls, and the extent to which partially dried droplets re-enter the hot areas around the air disperser. Fig. 2b shows that the lowest moisture content occurred when the inlet temperature increased from 150 to 220 °C. For spray drying in general, increasing the drying temperature results in a greater loss of water from the resultant powder because of the higher rate of heat transfer into the particles, which causes faster water removal (Krishnaiah *et al.*, 2014; Trujillo *et al.*, 2019). The powder moisture content decreases with increasing air inlet temperature and with decreasing drying air flow rate. A lower drying air flow rate causes an increase in the product sojourn time in the drying chamber and reinforces circulation effects. Increased residence times lead to a greater degree of moisture removal (Goula and Adamopoulos, 2004).

Finally, as seen from Fig. 2a, an increase in the rotary atomizer frequency from 60 to 90 Hz produced an increase in the outlet temperature and, therefore, a decrease in the product moisture content (Fig. 2b). The latter observation may be ascribed to the correlation of particle size and moisture content with the frequency of the rotary atomizer. According to the literature, higher atomizer wheel speeds and nozzle pressures decrease the droplet and therefore particle size (Huang and Mujumdar, 2008). According to previous reports, drying is facilitated by smaller particle sizes for two reasons. First, a larger surface area provides more surface area in contact with the heating medium and more surface area from which the moisture can escape. Second, smaller particles reduce the distance heat must travel to the center of the particles and reduce the distance through which moisture in the center of the particles must travel to reach the surface and escape (Goula and Adamopoulos, 2005).

3.2 Water activity

Fig. 2c shows the effect of the independent variables on the water activity of the dried product. An ANOVA indicates that the air flow shows a statistically significant effect ($p \leq 0.10$) on the water activity. It is evident from Fig. 2c that the water activity increases with the increment in the air flow from 537 to 619 kg·h^{-1} because the powder moisture content increases with decreasing drying air flow rate. The region with the lowest water activity corresponds to an inlet temperature of 150 °C, air flow of 537 kg·h^{-1}, and a rotary atomizer frequency of 90 Hz. In general, the water activity of the coffee extract powder ranged from 0.062 to 0.263 (Table 3); these values imply that the powders may have a longer shelf life, as there is less free water available for biochemical reactions (Norbrillinda *et al.*, 2016; Plazola *et al.*, 2019).
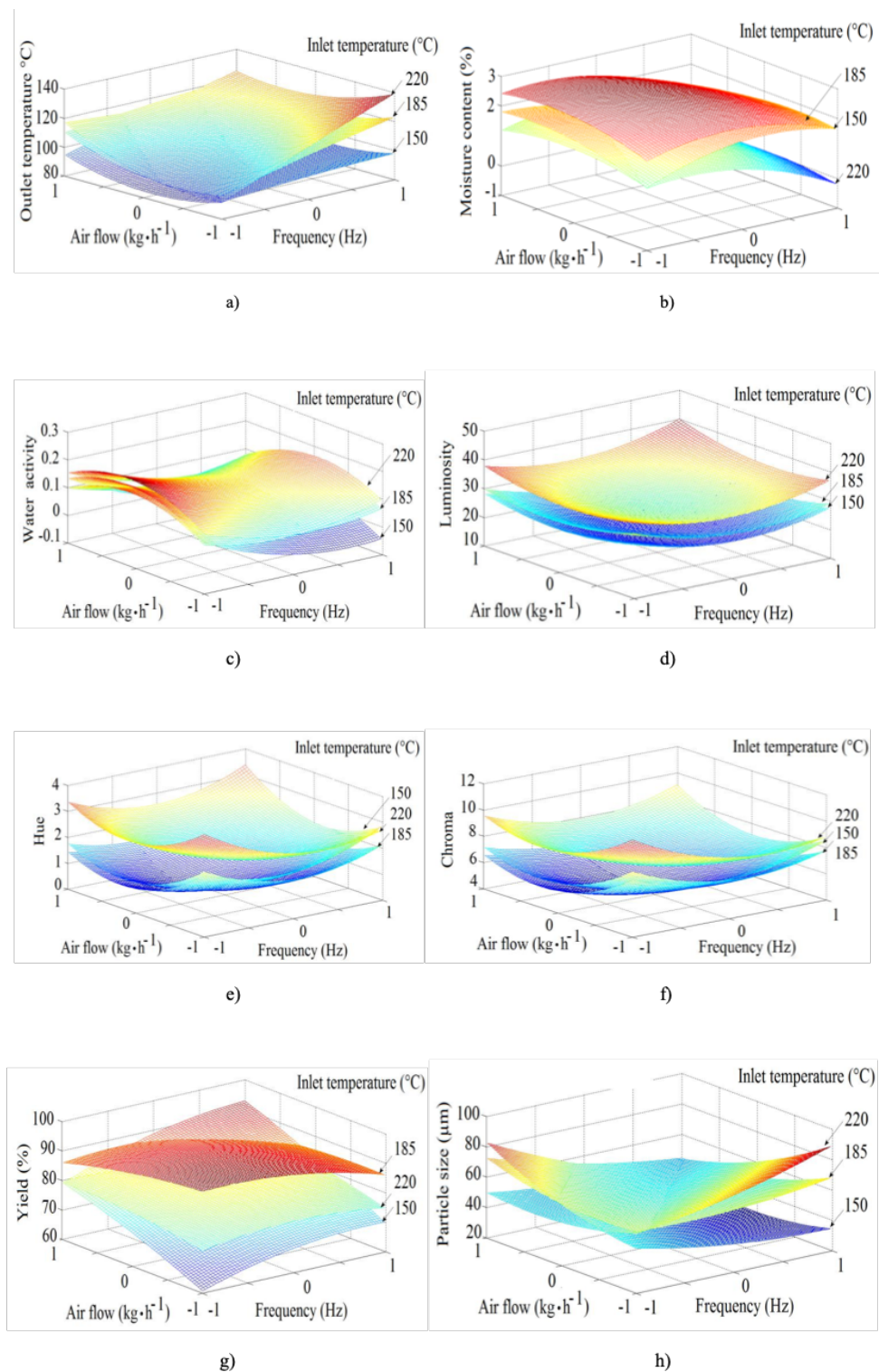
Fig. 2. 3D plot of: a) outlet temperature, b) Moisture content, c) Water activity, d) Luminosity, e) Hue, f) Chroma, g) Yield, and, h) Particle size as a function of inlet temperature, air flow, and frequency of the rotary atomizer.

Fig. 3. Samples of coffee powder at different drying conditions.

3.3 Color

Food color is one of the most important sensory attributes that are affected by many factors during spray drying, such as the air conditions (temperature and flow rate), feed conditions (enzyme inactivation, additives, and feed rate), and atomization speed, among other factors (Krishnaiah *et al.*, 2014). According to the results, the luminosity was significantly affected ($p \leq 0.10$) by the frequency of the rotary atomizer. Fig. 2d shows that the luminosity of the powders increased as the inlet temperature and air flow increased from 150 to 220 °C and from 537 to 691 kg·h^{-1}, respectively. The increasing value of L indicates that the powder product turned brighter, as shown in Fig. 3 (Exp. 1, 4, 10, 15). A similar effect on the lightness of powder was observed by Mishra *et al.*, (2013). During the spray drying of Amla (*Emblica officinalis*), they observed that increasing the inlet temperature from 125 to 200 °C produced a lighter powder than that produced at a lower inlet temperature. However, the present findings are contradictory to the behavior described by Krishnaiah *et al.*, (2014), who reported that an increase in the inlet temperature resulted in decreased lightness of the powders. This implied that the color of the powders became darker at higher inlet temperatures. On the contrary, the luminosity tended to decrease as the frequency of the rotary atomizer increased from 60 to 75 Hz. This implied that the color of the coffee powder became darker (Exp. 5, 6). Fig. 2e shows the effects of the inlet temperature, air flow, and frequency of the rotary atomizer on the hue parameter. As seen from Table 3, the hue values ranged from 0.61 to 3.96; these values indicate a red hue. According to Krishnaiah

et al., (2014), the hue angle measures the property of the color; an angle of 0° indicates a red hue, and angles of 270°, 180°, and 90° indicate blue, green, and yellow hues, respectively. In accordance with Fig. 2e, the highest hue angles were obtained when the inlet temperature increased from 150 to 220 °C. According to Quek *et al.*, (2007), when the inlet temperature increases, changes in the hue and chroma parameters can occur. Finally, Fig. 2f shows the influence of the independent variables on the chroma parameter. Chroma indicates the color saturation, which it is proportional to its intensity (Pérez *et al.*, 2018); the chroma values ranged from 5.25 to 11.22. As seen from Fig. 2f, the highest chroma value occurred at the inlet temperature of 220 °C. The same behavior was observed by Quek *et al.*, (2007) in the dry spraying of watermelon, who reported that an increment in the inlet air temperature from 145 to 175 °C, resulted in an increase in the chroma value from 22.02 to 31.09, as a result of in increment in the b values and a decrement in the a values. The chroma parameter of coffee powder tended to decrease slightly as the frequency of the rotary atomizer increased from 60 to 90 Hz, and it tended to decrease as the air flow increased.

3.4 Yield

Although a greater efficiency of heat and mass transfer processes occurs when higher inlet air temperatures are used (Tonon *et al.*, 2008), the highest production of coffee powder was obtained at an inlet temperature of 150, air flow of 691 kg·h^{-1}, and a rotary atomizer frequency of 90 Hz (Table 3, Exp. 6). An ANOVA shows that the frequency of the rotary atomizer affected the process yield significantly ($p \leq 0.10$). Fig. 2g shows that the yield tended to increase as the air flow and frequency of the rotary atomizer increased from 537 to 691 kg·h^{-1} and from 60 to 90 Hz, respectively. This result is expected because under these conditions, the dried product had the highest final moisture content (Fig. 2b). Similar findings were reported by Domínguez *et al.*, (2018); their results demonstrated that the production of dry cheese whey increased as the final moisture content increased. Accordingly, Chávez *et al.*, (2014) reported that at lower outlet temperatures (70 °C) and higher atomizer speeds (30,000 rpm), a higher powder yield was achieved (76%). However, Huang and Mujumdar, (2008), found that the amount of product collected from the drying chamber decreased when the atomizer rotating speed increased from 5,500 to 14,000 rpm.

The reason for this is that fine particles are obtained when the atomizer speed increases. Therefore, the fine particles are easily caught by the drying air and are collected from the cyclone to the container.

3.5 Particle size

An ANOVA revealed that the inlet air temperature, air flow, and frequency of the atomizer did not significantly affect ($p \geq 0.10$) the particle size of the coffee powder. As seen from Fig. 2h, the highest particle size occurred when the frequency of the rotary atomizer was increased from 60 to 90 Hz at the inlet temperatures of 185 and 220 °C. The present findings are contradictory to the results obtained by Huang and Mujumdar, (2008), who reported that an increase in the atomizer speed from 5,500 to 14,000 rpm resulted in a decrease in the particle size from 130.37 to 94.56 μm. The literature clearly demonstrates that in spray drying, higher atomizer wheel speeds and nozzle pressures decrease the droplet and therefore particle size (Goula and Adamopoulos, 2005). The probable reason for the increment in the particle size of coffee powder may be ascribed to the increase in the drying air temperature. According to Walton, (2000), increasing the drying air temperature generally produces an increase in the particle size caused by particle inflation-ballooning or puffing, and is particularly common in skin-forming materials. A similar behavior was observed by Kurozawa *et al.*, (2009) for chicken meat powder. Their results demonstrate that the particle size was affected positively by the air temperature; an increase in the inlet air temperature from 132 to 180 °C resulted in larger particles. However, the particle size showed a tendency to increase as the air flow increased from 537 to 691 kg·h^{-1} at inlet temperatures of 150 and 185 °C. An increment in the drying air flow rate causes a decrement in the product sojourn time in the drying chamber. According to Kurozawa *et al.*, (2009), drying under conditions that result in faster drying rates produces larger particles than drying under conditions that result in slower drying. On the contrary, an increment in the residence time leads to a greater degree of moisture removal. The powder particle size depends upon the degree of moisture removal during drying. In a standard system, the percentage increase in the size is inversely proportional to the percentage decrease in the moisture (Goula and Adamopoulos, 2004). However, in this case, the moisture content increased as the particle size increase. As mentioned before, high drying air temperatures generally result

in increased particle size. The particle size increased as the inlet temperature increased 150 to 185 °C. The larger surface area of smaller particles provides more surfaces from which the moisture can escape, as shown in Fig. 2b. In this case, increasing the air flow may produce an increase in the particle size of the product due to an increase in the inlet temperature.

3.6 Sorption isotherms

The effects of the independent variables on the sorption isotherms of coffee powder are shown in figs. (4)-(6). The obtained isotherms correspond to the sigmoid form and to type-III isotherms according to the classification by Labuza and Altunakar, (2007) and Yang *et al.*, (2008), where they proposed that dried food products usually show isotherms of type II or III. Food systems composed mainly of crystalline components such as sugars and salt are represented by type-III isotherms. As seen from Fig. 4, the highest water sorption occurred when the inlet temperature decreased from 220 to 150 °C. However, having the highest moisture content does not mean that the structural properties of coffee will be the same. According to the literature, heat treatments usually decrease the water binding of products. For this reason, dehydration at 220 °C can cause damage to the original structure; in this case, sufficient water cannot be absorbed and the rehydration is incomplete. According to Jimenez *et al.*, (2017) a higher moisture content for the same water activity value shows that the capillaries in the food structure close or contract during the drying process. This makes it more difficult, and impossible in many instances, for water to reenter the structure. This leaves a larger amount of water available and increases the water activity value.
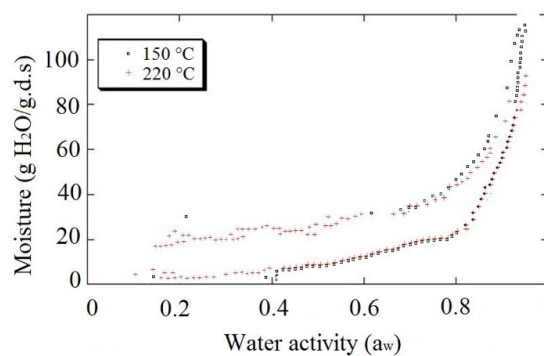
Fig. 4. Sorption isotherm of dehydrated coffee at different inlet air temperatures.
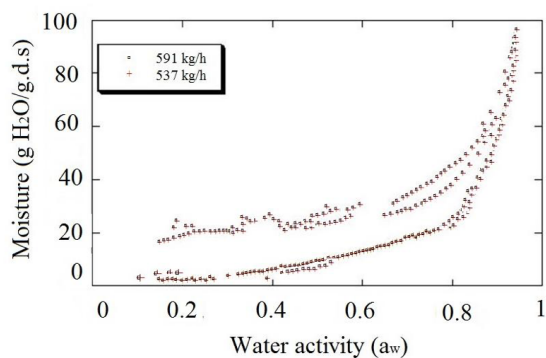
Fig. 5. Sorption isotherm of dehydrated coffee at different air flow rates.
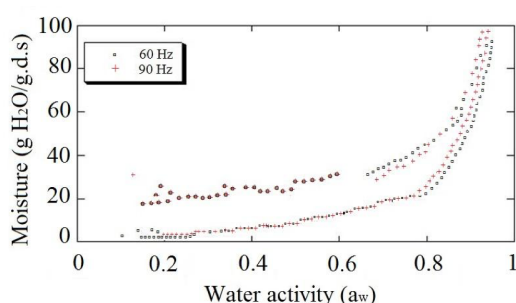

Fig. 6. Sorption isotherm of dehydrated coffee at different frequencies of the rotary atomizer.

When desorption and adsorption curves of a food material are drawn on isotherm graphs and the lines do not overlap, this is known as moisture hysteresis (Kaya and Öner, 1996; Farahnaky and Kamali, 2015). Figs. 5 and 6 show that the air flow and the rotary atomizer frequency did not affect the water sorption of the coffee powder. However, a broad hysteresis was observed when the air flow decreased from 691 to 537 kg·h^{-1} (Fig. 7a and Fig. 7b). The probable

reason for this behavior may be ascribed to the moisture removal during the drying process. The powder moisture content decreased with decreasing drying air flow rate. A lower drying air flow rate causes an increase in the product sojourn time in the drying chamber and reinforces circulation effects (Oakley and Bahu, 1991, Filková *et al.* 2014). Increased residence times lead to a greater degree of moisture removal. Therefore, damage to the original structure can occur. Fig. 7c and Fig. 7d clearly show a decrease in the hysteresis with increased air flow rate; therefore, a low degree of damage to the internal structure can be inferred. According to Labuza and Altunakar, (2007), if a moist low-a_w product is desired, a large desorption hysteresis would be beneficial because there would be more water at the same a_w. However, at the same a_w, a higher moisture content also results in a greater rate of loss for certain chemical reactions, thereby reducing the shelf life, which is undesirable. In this case, a low desorption hysteresis is desired, not only because the structural properties of the coffee will be similar to the original product, but also because the shelf life will increase owing to the low water activity values.

3.7 GAB and BET models

Table 5 shows the parameters calculated by the BET and GAB models. The degree of adjustment of each model was evaluated based on the coefficient of determination R^2. It was evident that the GAB model presented a better adjustment, with the highest R^2 values from 0.9976 to 0.9989, than the BET model, which generally holds only for a limited range of a_w. It should be noted that this a_w range of applicability is between 0 and 0.55; above the upper limit, the results deviate from a straight line when plotted as a linear equation.

Table 5. Parameters calculated by BET and GAB models.

Model	X_1		X_2		X_3	
BET	(-1)	-1	(-1)	-1	(-1)	-1
C	0.0067	0.1449	0.1449	0.0157	0.1449	0.007
m_0	1.1758	6.8887	6.8878	4.4728	6.8878	1.3597
R^2	0.9243	0.9086	0.9086	0.8238	0.9086	0.9963
GAB						
C	3.6324	2.5634	2.5634	1.8471	2.5634	2.6999
K	1.0166	0.99	0.99	0.9893	0.99	0.9908
m_0	4.5219	6.0533	6.0533	6.4566	6.0533	6.5917
R^2	0.9976	0.9985	0.9985	0.9986	0.9985	0.9989

X_1= Inlet air temperature (°C), X_2= Air flow (kg·h^{-1})
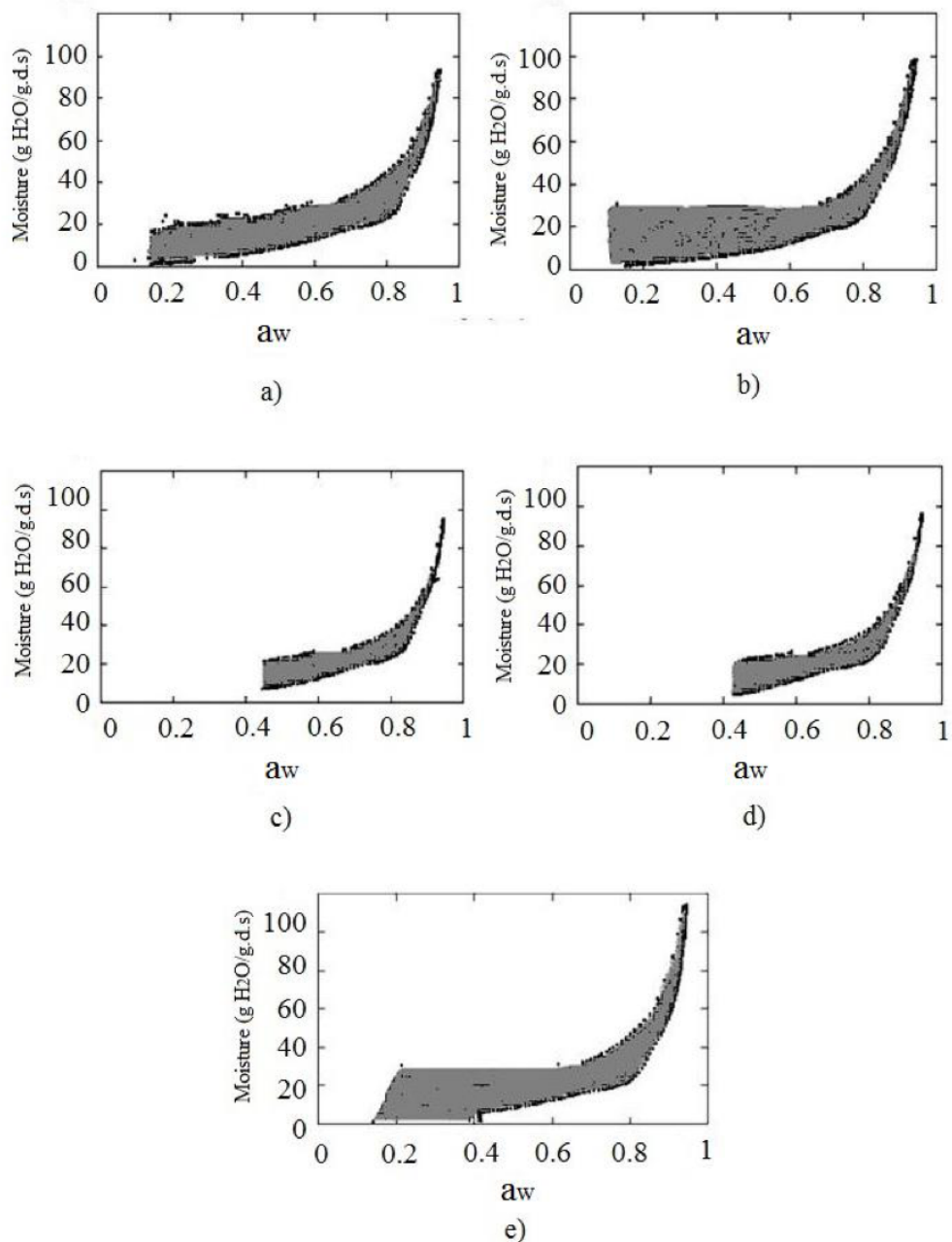X_3= Frequency of the atomizer (Hz).

Fig. 7. Hysteresis of dehydrated coffee at different drying conditions: a) 220 °C, 60 Hz, 537 kg/h, b) 220 °C, 90 Hz, 537 kg/h, c) 220 °C, 90 Hz, 691 kg/h, d) 220 °C, 60 Hz, 691 kg/h, e) 150 °C, 60 Hz, 537 kg/h.

On the contrary, the GAB equation has been found to adequately represent the experimental data in the a_w range of 0 to 0.95 for most foods of practical interest. The GAB and BET models are based on the same principles of monolayer coverage; however, the GAB model introduced an additional degree of freedom (an additional constant, k), with which the model has greater versatility (Labuza and Altunakar, 2007; Ramírez *et al.*, 2014). The monolayer moisture content, m_0, and the energy constant, C_s, obtained from the BET model ranged from 1.1758 to 6.8887 and from 0.0067 to 0.1449, respectively. At this

monolayer moisture content, the rates of quality loss are negligible. The value of the monolayer (m_0) is of particular importance, as it indicates the amount of water that is strongly adsorbed to specific sites and is considered as the value at which a food is the most stable against microbial spoilage (Pavón *et al.*, 2015). For the GAB model, the value of C_s ranged from 1.8471 to 3.6324 and the values of the additional constant k were close to 1. According to the literature, the value of *k* varies from 0.7 to 1 for many food materials. However, in some instances, *k* values greater than one are reported, such as for freeze-dried raspberries ($k = 1.024$) (Khallouﬁ *et al.*, 2000) and for fresh grapes and apricots ($k = 2.243$ and 1.049, respectively) (Kaymak and Gedik, 2004). *k* values greater than one are mainly due to the nonlinear GAB model taking only water content and water activity as inputs (Djendoubi, 2012). Although the moisture sorption values for the GAB model ranged from 4.5219 to 6.5917, these did not affect the quality of the product. According to the results, the GAB model was adequate to predict the moisture sorption behavior. Some advantages of the GAB model are that it has a viable theoretical basis; it describes sorption behavior of most foods, from 0 to 0.95 a_w; it has a mathematical form with only three parameters, making it highly amenable to engineering calculations; and its parameters have physical meaning in terms of the sorption processes. In this sense, it is important further research on sorption isotherms and thermodynamic approaches at different temperatures in order to analyze the optimal processing and storage conditions of coffee powder, thus avoiding undesirable modifications and enhancing the product's shelf life.

Conclusions

In this work, the effects of the spray drying conditions on the moisture content and particle size of coffee extract were studied. The moisture content, color parameters, yield, and particle size were significantly influenced ($p \leq 0.10$) by the frequency of the rotary atomizer. The moisture content and water activity of the coffee powder were reduced sufficiently to ensure microbiological and chemical stability. The moisture content and water activity values of the coffee extract powder ranged from 0.37 to 2.78 and from 0.062 to 0.263, respectively; these values imply that the powders may have a longer shelf life, as there is less free water available for biochemical reactions.

The luminosity tended to decrease with increasing of rotary atomizer frequency. Therefore, the color of the coffee powder became darker. The highest production of coffee powder was obtained at an inlet temperature of 150 °C, air flow of 691 kg·h^{-1}, and a rotary atomizer frequency of 90 Hz. Under these conditions, the dried product had the highest final moisture content. The particle size increased as the air flow increased from 537 to 691 kg·h^{-1} at the inlet temperatures of 150 and 185 °C. The air flow and rotary atomizer frequency did not affect the water sorption of the coffee powder. A broad hysteresis was observed when the air flow decrease from 691 to 537 kg·h^{-1}. A decrease in the hysteresis was observed with an increase in the air flow rate. The low desorption hysteresis indicated that the structural properties of the coffee would be similar to those of the original product. The GAB model was the most adequate, because it describes sorption behavior in the aw range from 0 to 0.95. The GAB model presented a better adjustment, with the highest R^2 values from 0.9976 to 0.9989, than the BET model, which generally holds only for a limited range of aw.

Nomenclature

FAO	Food and Agricultural Organization of the United Nations
BET	Brunauer-Emmet-Teller isotherm
m_0	Monolayer moisture content
C_s	Energy constant
GAB	Guggenheim-Anderson-de Boer isotherm
a_w	Water activity
k	constant
d.b	Dry basis
L	Whiteness-darkness
a	Redness-greenness
b	Yellowness-blueness
H	Hue
C	Chroma
$\tan^{-1}$	Arctangent
Y_k	Response variables

f_k	Mathematical functions
X_1	Inlet air temperature (°C)
X_2	Air flow (kg·h^{-1})
X_3	Frequency of the rotary atomizer (Hz)
RSM	Response surface methodology
b_{k0}	Regression coefficient
b_{ki}	Linear regression coefficient
b_{kii}	Quadratic regression coefficient
b_{kij}	Interaction coefficient
X_i's	Coded independent variables
ANOVA	Analysis of variance
R^2	Coefficient of determination

References

Burmester, K., Fehr, H. and Eggers, R. (2011). A comprehensive study on thermophysical material properties for an innovative coffee drying process. *Drying Technology 29*, 1562-1570.

Chávez, R.A., López, M.I.G., Gómez, L.J., Luna, S.G., Ortíz, B.R.I. and Andrade, G.I. (2014). Optimization of *Agave tequilana* Weber var. Azul Juice spray drying process. *Journal of Chemistry 915941*, 1-10

Domínguez, N.A., Cantú, L.D., Ragazzo, S.J.A., Andrade, G.I. and Luna, S.G. (2018). Energy requirements and production cost of the spray drying process of cheese whey. *Drying Technology 36*, 597-608.

Djendoubi, M.N., Bonazzi, C., Boudhrioua, N., Kechaou, N. and Courtois, F. (2012). Infuence of sugar composition on water sorption isotherms and on glass transition in apricots. *Journal of Food Engineering 111*, 403-411.

Farahnaky, A. and Kamali, E. (2015). Texture hysteresis of pistachio kernels on drying and rehydration. *Journal of Food Engineering 166*, 335-341.

Faria, F.M.L., Carregari, P.T., De Souza, A.C. and Telis, J. (2016). Sorption isotherms and thermodynamic properties of grated parmesan cheese. *Food Science and Technology 51*, 250-259.

Filková, I., Huan, L.X., and Mujumdar, A.S. (2014). Industrial spray drying systems. In: *Handbook of Industrial Drying*, (A.S. Mujumdar, ed.), Pp. 191-226. CRC Press, Boca Raton, FL. Food and Agricultural Organization of the United Nations. (2015). Coffee. Editorial FAO, ROMA.

Goula, A.M. and Adamopoulos, K.G. (2004). Spray drying of tomato pulp: effect of feed concentration. *Drying Technology 22*, 2309-2330.

Goula, A.M. and Adamopoulos, K.G. (2005). Spray drying of tomato pulp in dehumidified air: II. The effect on powder properties. *Food Engineering 66*, 35-42.

Hernández, A.A., Casillas, R.B.C., Cocotle, R.Y., Puebla, H. and Hernández, M.E. (2019). Monitoreo del tostado de café usando la transformada de Fourier 2D de imágenes. *Revista Mexicana de Ingeniería Química 18*, 231-240.

Hernández, C.J.G., Mújica, P.H., Welti, C.J., Spatafora, S.A.S., and Valdez, F.A. (2019). Sorption behavior of citric pectin films with glycerol and olive oil. *Revista Mexicana de Ingeniería Química 18*, 487-500.

Huan, L.X. and Mujumdar, A.S. (2008). The effect of rotary disk atomizer RPM on particle size distribution in a semi-industrial spray dryer. *Drying Technology 26*, 1319-1325.

Jimenez, S.D.E., Calderón, S.M., Picart, P.L., Luna, S.G., Ortiz, B.R.I., Bautista, R.P.U. and Ragazzo, S.J.A. (2017). Effect of addition of native agave fructans on spray-dried chayote (*Sechium edule*) and pineaple (*Ananas comosus*) juices: rheology, microstructure, and water sorption. *Food and Bioprocess Technology 10*, 2069-2080.

Kaya, S. and Öner, M.D. (1996). Water activity and moisture sorption isotherms of Gaziantep cheese. *Journal of Food Quality 19*, 121-132.

Kaymak, E.F and Gedik, A. (2004). Sorption isotherms and isosteric heat of sorption for grapes, apricost, apples and potatoes. *LWT-Food Science and Technology 37*, 429-438.

Khalloufi, S., El-Maslouhi, Y. and Ratti, C. (2000). Mathematical model for prediction of glass transition temperature of fruit powders. *Journal of Food Science 65*, 842.848.

Khetra, Y., Kanawjia, S.K. and Puri, R. (2017). Effect of sodium and its substitution whit potassium on desorption and thermodynamic properties of cheddar cheese. *Journal of Food Processing and Preservation 41*, e12991

Krishnaiah, D., Nithyanandam, R. and Sarbatly, R. (2014). A critical review on the spray drying of fruit extract: effect of additives on physicochemical properties. *Food Science and Nutrition 54*, 449-473.

Kurozawa, L.E., Morassi, A.G., Vanzo, A.A., Park, K.J. and Hubinger, M.D. (2009). Influence of spray drying conditions on physicochemical properties of chicken meat powder. *Drying Technology 27*, 1248-1257.

Labuza, T.P. and Altunakar, B. (2007). Water activity prediction and moisture sorption isotherms. In: *Water Activity in Foods*, (B. Gustavo., F. Anthony., S. Shelly., and L. Theodore, eds.), Pp 109-154. IFT PRESS, Iowa, USA.

Lantigua M.B., Molina E.I., Reineccius G.A., Hernández O.L. and Pino J.A. (2011). Influence of spray-dryer air temperatures on encapsulated mandarin oil. *Drying Technology 29*, 520-526.

Norbrillinda, M.T., Mahanom, H., Elyana, N.N. and Farina, N.I. (2016). Optimization of spray drying process of *Sargassum muticum* color extract. *Drying Technology 34*, 1735-1744.

Oakley, D.E. and Bahu, R.E. (1991). Spray or gas mixing behavior within spray dryers. In: *Drying'91*, (A.S. Mujumdar and I. Filková, eds), Pp 303-313. Elsevier Science Publishers, Amsterdam, the Netherlands.

Pascual, P.L.A., Alamilla, B.L., Gutiérrez, L.G.F., Azuara, E. and Flores, A.E. (2017). Predicción de condiciones de almacenamiento de alimentos deshidratados a partir de una isoterma de adsorción de vapor de agua. *Revista Mexicana de Ingeniería Química 16*, 207-220.

Pavón, G.L.M.A., Gallardo, R.R., Román, G.A., Carrillo, N.H., Rodríguez, H.M.E., Guadarrama, L.A.Y., and Pérez, A.C. (2015). Moisture sorption properties and storage stability conditions of a nutraceutical system microencapsulated by spray drying. *Revista Mexicana de Ingeniería Química 14*, 601-613.

Pérez, G.B., García, Z.J.C., Ruíz, P.V.M., Téllez, M.D.I., García, P.S., Guzmán, G.R.I. and Mora, E.R. (2018). Biofunctionality, colorimetric coefficients and microbiological stability of blackberry (*Rubus fructicosus* var. Himalaya) juice under microwave/ultrasound processing. *Revista Mexicana de Ingeniería Química 17*, 13-28.

Plazola, J.C.P., Pérez, P.V., Pereyra, C.S.C., Alamilla, B.L., and Ortiz, M.A. (2019). Microencapsulation of biocompounds from avocado leaves oily extracts. *Revista Mexicana de Ingeniería Química 18*, 1261-1276.

Quek, S.Y., Chok, N.K. and Swedlund, P. (2007). The physicochemical properties of spray-dried watermelon powder. *Chemical Engineering and Processing 46*, 386-392.

Ramírez, M.M., Cruz y Victoria, M.T., Vizcarra, M.M.G. and Anaya, S.I. (2014). Determinación de las isotermas de sorción y las propiedades termodinámicas de harina de maíz nixtamalizada. *Revista Mexicana de Ingeniería Química 13*, 165-178.

Roustapour, O.R., Hosseinalipour, M. and Ghobadian. (2006). An experimental investigation of lime juice drying in a pilot plant spray dryer. *Drying Technology 24*, 181-188.

Schmidt, S.J. and Won Lee J. (2012). Comparison between water vapor sorption isotherms obtained using the new dynamic dewpoint isotherm method and those obtained using the standard saturated salt slurry method. *International Journal of Food Properties 15*, 236-248.

Sinija, V.R. and Mishra, H.N. (2008). Moisture sorption isotherms and heat of sorption of instant (soluble) green tea powder and green tea granules. *Journal of Food Engineering 86*, 494-500.

Solval, M.S., Sundararajan S., Alfaro, L. and Sathivel, S. (2012). Development of cantaloupe (*Cucumis melo*) juice powders using spray drying technology. *LWT-Food Science and Technology 46*, 287-293.

Thys, R.C.S., Noreña, C.P.Z., Marczak, L.D.F., Aires, A.G. and Olivera, F.C. (2010). Adsorption isotherms of pinhão (*Araucaria*

angustifolia seeds) starch and thermodynamic analysis. *Journal of Food Engineering 100*, 468-473.

Tonon, R.V., Brabet, C. and Hubinger, M.D. (2008). Influence of process conditions on the physicochemical properties of acai (*Euterpe oleraceae* Mart.) powder produced by spray drying. *Food Engineering 88*, 411-418.

Trujillo, C.L., Camacho, B.M., Cano, S.C., Duarte, V.M.A., Viveros, C.R. and Rosado, J.L. (2019). Development of an infant formula high in alpha-lactalbumin with only A$_2$ beta-casein by spray drying, designed to resemble the protein composition of human milk. *Revista Mexicana de Ingeniería Química 18*, 215-229.

Walton, D.E. The morphology of spray dried particles a qualitative view. (2000). *Drying Technology 18*, 1943-1986.

Yang, Z., Sousa-Gallagher, M.J. and Oliveira, F.A.R. (2008). Sorption isotherms and moisture sorption hysteresis of intermediate moisture content banana. *Journal of Food Engineering 86*, 342-348.

Zhang, L., Sun, D.W. and Zhang, Z. (2017). Methods for measuring water activity (a_w) of foods and its applications to moisture sorption isotherm studies. *Critical Reviews in Food Science and Nutrition 57*, 1052-1058.